Journal of Electroceramics, 14, 75–81, 2005

Low Loss Tungsten-Based Electrode Technology for Microwave Frequency BST Varactors

J.-P. MARIA,[1,*] B.A. BOYETTE,[1] A.I. KINGON,[1] C. RAGAGLIA[2] & G. STAUF[2]
[1]*Department of Materials Science and Engineering, North Carolina State University, Raleigh, 27695-7920, NC, USA*
[2]*Advanced Technology Materials, Inc., Danbury, CT 06810, USA*

Submitted January 16, 2004; Revised June 16, 2004; Accepted June 18, 2004

Abstract. Composite metallization stacks consisting of 1.5 μm W layers and 0.1 μm Ir layers have been developed for low series resistance electrode applications. These hybrid metallization layers are compatible with barium strontium titanate deposition and standard patterning/etching procedures. The multilayer stacks were prepared for use as bottom electrodes in microwave varactors based upon the electrically tunable dielectric barium strontium titanate. These low resistivity layers are critical for realizing low insertion loss devices, and overcome difficulties associated with delamination or hillocking in traditional noble metal layers. Controlling the oxygen content during BST deposition was necessary to achieve high-quality BST and a stable electrode stack. Using these metallization stacks and optimized deposition conditions, BST films with tan δ values below 0.007 and tunabilities of 2:1 were realized. These properties are comparable to those measured on typical Pt/BST/Pt/SiO_2/Si capacitors. Finally, a combination of reactive ion and wet chemical etching were used to demonstrate that the thick hybrid metallization layers are patternable using routine and manufacturable process methods.

Keywords: microwave, BST, electrode, ferroelectric, metallization

1. Introduction

Replacing semiconductor varactors with electrically tunable dielectrics is of technological interest given the potential improvements in high frequency loss, device reliability, and miniaturization [1]. The electrically tunable dielectric of greatest current interest is (Ba,Sr)TiO_3 with a composition and thickness adjusted such that the ferroelectric transition temperature is close to, but below the predicted operating ambient [2]. Producing metal-insulator-metal capacitors with BST dielectric layers has been routinely demonstrated, with loss tangent values $<1\%$ and tunabilites equal to or greater than 2:1. Though these loss tangents will yield dielectric Q values approaching 1000, total device Qs in this range have not been reported. In part, this results from the lack of a suitable electrode technology offering low dc resistance. The quality factor of a tunable capacitor can be expressed in the following manner:

$$\frac{1}{Q_{\text{total}}} = \frac{1}{Q_{\text{BST}}} + \frac{1}{Q_{\text{metal}}} = \tan\delta + \omega C_P R_S$$

where the contributions from the dielectric loss, capacitance, frequency, and series resistance can be separated. This behavior is graphically represented in Fig. 1. Note in Fig. 1 that for a 1 GHz, 1 pF capacitor, if a Q factor of 100 is desired, the metallization cannot supply more than 5 Ω of total resistance. For Pt electrodes, a 50 μm wide line prepared with the common 100 nm thickness with provide this resistance value in a length of only 250 μm. This example represents only a first order approximation of a complex system, however, it does accurately depict one limiting case where metallization loss provides the predominant influence [3]. To overcome this obvious limitation, lower resistivity structures are necessary. The simplest way to reduce the metal series resistance is through increasing the electrode thickness. Unfortunately, however, increasing the

*To whom all correspondence should be addressed. E-mail: jpmaria@ncsu.edu

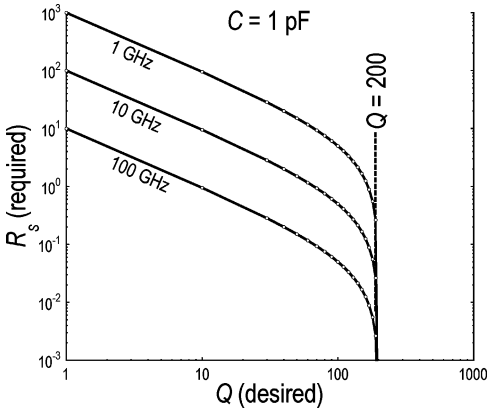

Fig. 1. The relationship between device series resistance and device quality factor. This plot corresponds to a 1 pF capacitance value, and a capacitor dielectric with a loss tangent of 0.005 (or a dielectric quality factor of 200).

thickness of commonly used Pt electrodes is technically problematic and commercially impractical. Problems stemming from metal-substrate thermal expansion mismatch make thick layers physically unstable during the high temperature excursions required for dielectric deposition and annealing. The two most common difficulties include Pt roughening (through a hillocking process) and Pt film delamination [4]. In addition, patterning thick Pt, i.e., multiple μm thicknesses, is difficult and time consuming. Finally, the expense associated with such large quantities of Pt makes the technology cost prohibitive, especially in RF or microwave devices where metallization areas can be large.

An alternative approach to reduced series resistance metallization involves hybrid combinations of noble-metal and base-metal layers. Ideally, a thick base-metal is used to carry current over long lateral distances thereby reducing overall resistance, and a thin top noble metal layer is used to provide a chemically inert interface and an appropriate BST nucleation surface. This investigation details the selection process of appropriate materials and the development of an acceptable deposition process to achieve this hybrid metallization solution.

2. Results and Discussion

2.1. Material Selection

To select the optimal material combination, a set of material property criteria was established. Table 1 lists

Table 1. Important characteristics of noble and base metals important for hybrid electrode stack design.

Noble metal	Base metal
Non-reactive with BST at high temperature	Oxidation resistant
Provides good BST nucleation surface	Conductivity of oxide
Patternable using wet chemicals or RIE	Good adhesion to SiO_2
Oxygen diffusion resistance	Low resistance Low thermal expansion Patternable with wet etchant

the most important requirements for both noble and base-metal components. For the noble metal, these include stability in contact with BST and patternability. Since the noble metal is envisioned to encompass only a thin surface layer, etching with either wet chemicals or reactive ion techniques are practical. The resistivity of the noble metal is not critical since this component will only carry the high frequency signal over a distance similar to the layer thickness: as such, the total resistance will be small even if the resistivity is appreciable. For the base metal, the most important requirements are low resistivity, low thermal expansion coefficients, and etchability. Small thermal expansion coefficients will minimize residual strains stemming from thermal expansion mismatch. This occurs because high resistivity Si, fused silica, and sapphire (the most common substrates for these applications) all have small CTE values when compared to traditional oxide dielectric metallization materials. Metal layers with the smallest thermal expansion coefficients will provide for the smallest residual strains and will in turn provide for improved thermophysical stability. Small resistivity values are important for minimizing total metal film thickness. If the metals do not have suitably high conductivity values, the layer thicknesses required to achieve appropriately low series resistance will necessitate device geometries with impractical aspect ratios. For instance, a coplanar waveguide cannot have a vertical thicknesses which approaches the spacing between ground and signal lines. Furthermore, a smaller metal thickness offers a smoother and generally more stable surface on which to prepare dielectric films. The base metal should also be patternable with a wet chemical etchant or a common dry etch process. This requirement comes from the difficulty, time, and expense of plasma etching many noble or refractory metal layers. Finally, the subject of

metal skin depth (δ) should be mentioned. To minimize resistance losses, the optimal thickness for a metallization line is three times the skin depth (which scales with the inverse root of frequency). For all conductors, the resistance/length of such a line would be identical, the areas, however are not. For copper and Pt lines At 100 GHz, the 3δ values would be 0.6 and 1.5 μm respectively. Thus one can appreciate, that even approaching the end of microwave bands, appreciable metal thicknesses are needed for minimization of conductor losses, and low resistivity metals offer more attractive dimensions.

No two materials can provide all criteria in Table 1, however, the combination of IrO_x and W provide the most reasonable compromises. Tungsten has a room temperature resistivity of 5.5 $\mu\Omega$-cm, a room temperature thermal expansion coefficient of 5.6 ppm/K, a metallically conducting oxide, and can be etched easily with concentrated peroxide at room temperature [5]. Ir has a room temperature resistivity of 6 $\mu\Omega$-cm, a metallically conducting oxide providing good oxygen diffusion resistance, but must be etched using plasma techniques. Alternatively, Pt has a room temperature resistivity of 9 $\mu\Omega$-cm, a thermal expansion coefficient of 9 ppm/K, and no known solid oxide phases [5]. Platinum has the additional advantage of being readily etched in aqua regia. Unfortunately, however, Pt is well known for its catalytic activity with O_2 and its subsequent transparency to O. As such, we eliminate Pt from our comparison. Combinations of Ir and W are not expected to form low temperature intermetallic phases and do not exhibit extensive solid-solid solubility [6]. Clearly the oxide of tungsten is volatile at typical thin film processing temperatures, but with the presence of the Ir or IrO_2 surface layers, W oxidation may be thwarted. Care must however be taken as the $Ir/IrO_2/O_2$ equilibrium condition is in many cases close to the BST deposition ambient. Given the IrO_2 reduction possibility, the oxygen pressure cannot be reduced arbitrarily as the oxygen diffusion barrier property can be compromised. If a reduced oxygen pressure envelope favoring IrO_x and high quality BST can be found, compatibility between thick electrodes and tunable oxides is possible.

2.2. *Process Optimization*

BST chemical vapor or chemical solution deposition is typically carried out in conditions of large excess oxidant concentrations. Such conditions are used to ensure that organic removal is as efficient and complete. In the case where hybrid substrates are used, however, a gross excess of oxidant can be detrimental. For the case of the hybrid metal stack Ir/W, the ideal oxygen pressure would be enough to fully combust the MOCVD organic carrier, and enough to keep the Ir surface fully oxidized. Though it is often assumed that Ir is an easily oxidized cation, evaluation of the pressure dependent thermodynamics reveals the ease of IrO_2 reduction during common BST deposition conditions [7]. Figure 2 shows an oxygen pressure—temperature phase diagram for the system Ir-IrO_2-O_2. With this construction, the similarity in free energy of the oxide and metal phases under typical thin film deposition conditions can be appreciated. The most effective diffusion barrier is IrO_2, but the thermodynamic data reveals the potential difficulty in achieving this stoichiometry. Alternatively, large excesses of oxygen should be avoided (even though a diffusion barrier is present) since oxygen penetration in any scenario will be finite. Avoiding even small quantities of WO_3 is of particular concern given the volatility of WO_3. Production of a sub-surface gaseous phase will lead to efficient electrode failure. To determine this optimization, the MOCVD BST deposition conditions containing the smallest quantity of oxidant (and still capable of decomposing the organic precursor component) were determined. The optimization was

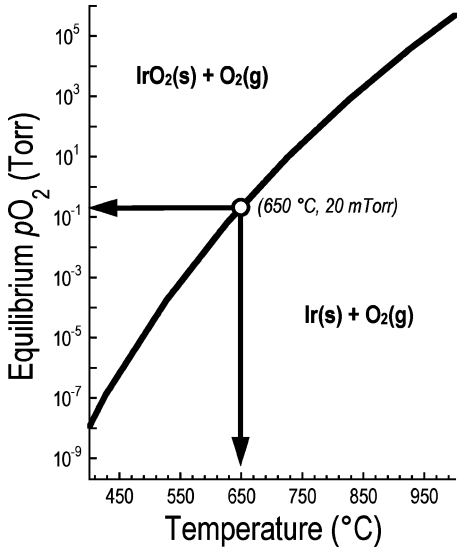

Fig. 2. Pressure-Temperature phase diagram for the Ir (s)–O_2 (g)–IrO_2 (s) system.

monitored using a combination of electrical characterization and surface imaging, in addition to an investigation of W/Ir layers exposed directly to atmospheric conditions as a function of oxygen pressure and temperature. Note that this process should be amenable to physical vapor deposition methods. A necessity in this case, however, would be to understand and appropriately control the action of the highly reactive oxygen species that can be found in vapor plasmas.

The initial step in process optimization was an investigation the electrode stack response to high temperature in both oxidizing and reducing conditions. Stacks of 1.5 μm W and 0.1 μm Ir were prepared by dc magnetron sputtering in a UHV chamber with a base pressure of 8×10^{-8} Torr. For both materials a sputtering power of 250 watts was employed on a 4 inch diameter metal foil target. The sputtering pressure was 30 mTorr and a target-to-substrate distance of 5 cm was used. The sputtering rate for W was 2.1 nm/second while the sputter rate for Ir was 1 nm/second. In all cases, thickness was determined by profilometry along masked film edges. The metal stack was then annealed at temperatures mimicking the BST deposition conditions. Note that the actual oxygen partial pressure during the BST deposition is difficult to determine given the simultaneous delivery of oxidant, metaloganic precursor, and the decomposition reaction which tends to locally reduce pO_2. Consequently, a 30 minute exposure to a partial oxygen pressure of 10^{-2} and a temperature of 700°C was used to estimate this process. Optical imaging at 1000× with Normarsky contrast revealed no significant roughening, peeling, or obvious signs of reaction after this annealing process. Given this success, BST depositions were attempted on similar Ir/W stacks. Typically, BST MOCVD depositions are conducted in an atmosphere containing large excess of oxidizing species to minimize the residual carbon content. In the case of normal Pt bottom electrodes, this is not problematic given the stability of Pt. In the present case where an oxidizable thick metal is buried under the thin noble metal skin, since some degree of oxygen diffusion is inevitable, minimizing the oxidation power of the deposition ambient while still maintaining high quality dielectric films is needed. BST films were prepared using a traditional liquid delivery system with systematically varied oxygen flow rates to determine the optimal deposition condition, details are available in the references [8, 9]. The total flow rates were held constant, but the ratio of carrier gas to oxygen was varied. The total gas flow was 800 sccm, the temperature stage in the reactor was 650°C, and the substrates were quarter sections of 150 mm Si wafers with 20 nm of thermal oxide under the hybrid metal stacks. Calibrated X-ray fluorescence measurements of the BST films were collected—the Ba/Sr ratio was between 1.1 and 1.07 and there was ∼4% excess Ti in all samples. BST thicknesses were also determined using the fluorescence method, in all cases the Dielectric thickness was between 100 and 110 nm. Figure 3 shows

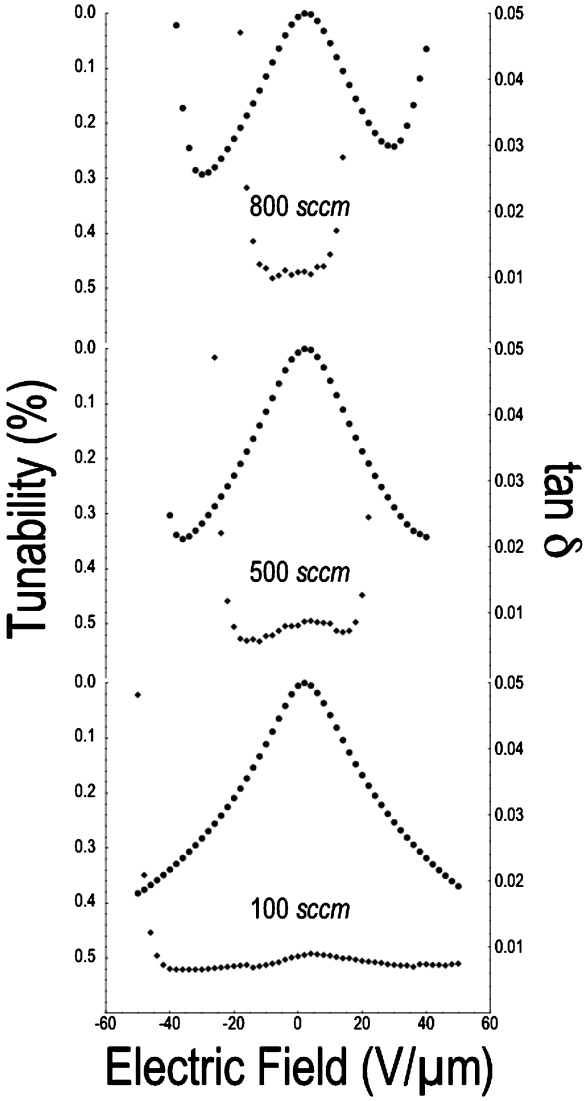

Fig. 3. Capacitance-field curves for BST films prepared as a function of oxygen flow rate during MOCVD deposition. This figure demonstrates the increase in voltage tolerance and decrease in loss tangent for BST films prepared with decreasing oxygen flow.

a series of capacitance-field curves for BST films prepared with different levels of oxygen flow. As seen in the figures, with reduced oxygen content the electric fields that can be tolerated increase dramatically, and ultimately, when the oxidant flow rate is reduced to near 100 sccm, film quality consistent with material prepared on Pt electrodes is produced. Tunabilities approaching 2:1 and loss tangent values fall below 1%. It is interesting to note that the tunability curves and the loss tangent values at low fields are consistent for all preparation conditions suggesting that the BST films are not strongly dependent on oxygen flow within the range investigated, and that a microstructural effect provides the predominant influence. To investigate this hypothesis, films prepared in high oxygen flow conditions that exhibited rapidly increasing loss tangent values under low electric fields were etched from the electrode stack such that the electrode structure underneath could be imaged directly in an electron microscope. Figure 4 shows such an image at two magnifications. The likely source of breakdown becomes apparent, and can be attributed to small protuberances scattered across the bottom electrode surface. We relate these structures to localized oxidation of the underlying tungsten and subsequent volatilization of WO_3 gas. Note that this result suggests a kinetic limitation based on a 100 nm Ir metal film (with an oxidized surface) at the onset of BST deposition. If additional thickness of Ir were used, or perhaps phase pure IrO_2, higher oxygen flow rates may be possible. Note however, that patternability remains an important concern, thus making Ir with an IrO_2 skin the preferable choice.

To complete the physical analysis of these film sets, X-ray diffraction analysis was conducted. Data for a BST film prepared on a 1.5 μm W/0.1 μm Ir stack is shown in Fig. 5. The only identifiable peaks are associated with BST and W metal. It is somewhat surprising that diffraction events from IrO_2 are not seen. This suggests that IrO_2 exists only as a sparingly thin surface layer. Note that Ir is isostructural and of similar d-spacing to W thus its reflections are masked by the much thicker W lines.

When processing oxide dielectric films under reduced oxygen pressure conditions, there is always some concern of uncontrolled defect populations attributable to non-stoichiometry in the anion sublattice. Measuring

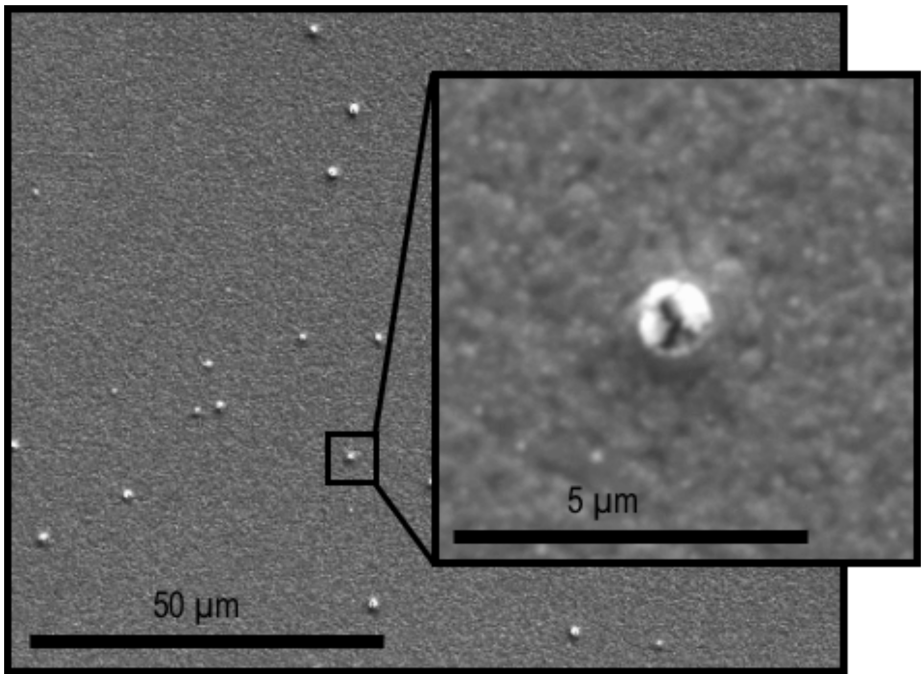

Fig. 4. Scanning electron microscope images of an IrO_x/W bottom electrode surface. This surface corresponds to the hybrid electrode surface after BST deposition. The BST thin film was etched from the stack using 1% HF solution such that the electrode surface could be imaged directly. The inset corresponds to a magnification of an electrode defect attributed to substrate oxidation and subsequent WO_3 (g) volatilization.

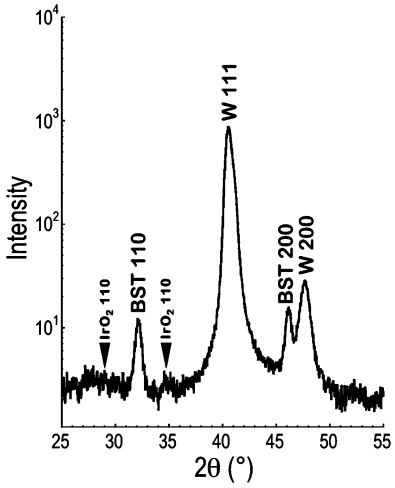

Fig. 5. Capacitance-frequency curves for a BST film prepared on a W/Ir stack under the optimized oxygen flow during MOCVD deposition. Note that the increase in loss tangent above 300 kHz corresponds to the frequency limitation of the test fixture as opposed to a strong dielectric dispersion in the BST film.

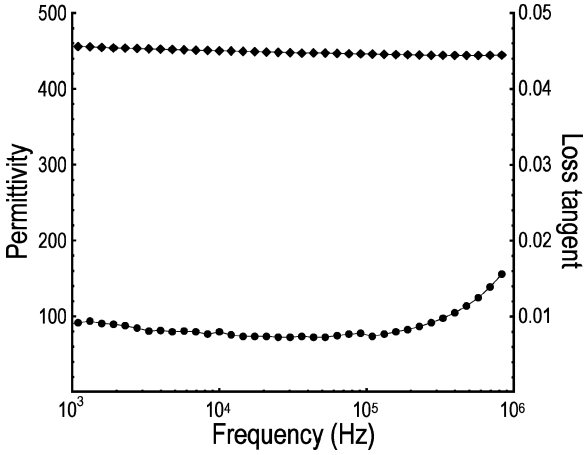

Fig. 6. An optical micrograph of etched 1.5 μm W/0.1 μm IrO_x electrode stack. 10 μm features are featured in this image.

the frequency dependence of the impedance is one method by which this condition may be detected since such defect concentrations can manifest in dielectric dispersion. Figure 6 shows the frequency dependence of the permittivity for a sample prepared under the optimized 100 sccm flow rate. The degree of dispersion observed with both capacitance and loss tangent is within experimental accuracy. Note that the variation in loss tangent above 200 kHz is associated with a finite fixture impedance as opposed to a material dependence. Consequently we hypothesize that the reduced oxygen atmosphere in the MOCVD reactor does not impart a noticeable effect in our dielectric.

The final issue of importance regarding thick electrode technology is the ability to etch the component materials in a reasonable manner. Previous authors have demonstrated the ability to prepare BST films on thick Pt metal layers with interleaved adhesion/stabilizing layers of either IrO_2 or TiN, however the expense and difficulty in etching such stacks makes them impractical for all but scientific investigation. The present technology of W/Ir stacks, however can be patterned in a straight forward manner using one lithographic step. Once the appropriate photoresist pattern is applied to the metal surface, a brief reactive ion etch can be used to pattern the thin 100 nm Ir surface layer. In the present case, a mixture of Ar and SF_6 was used during a 12 minute etch process. Once the Ir layer is patterned, the sample can be immersed in a room temperature concentrated peroxide solution (30%). This solution will etch the 1.5 μm W layer by an oxidation process in approximately 45 minutes. Higher temperatures can be used to increase the etching rate, however degradation of the peroxide becomes rapid. Figure 7 shows a Normarski optical image of a fully etched W/Ir electrode stack, the pattern corresponding to bottom electrodes for MIM microwave test structures. In this figure, the ability to produce feature sizes below 10 μm is identified.

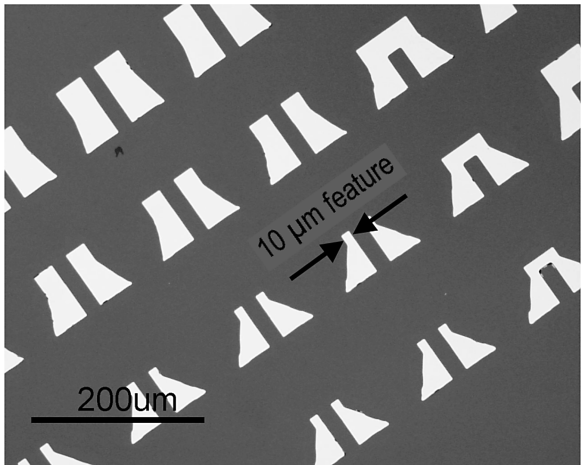

Fig. 7. Optical microscope image of patterned W/Ir electrode stack. Light regions correspond to bottom electrode structures of three level ground-signal-ground microwave test structures.

3. Summary

The authors have demonstrated a thick electrode technology consistent with the demands of high frequency devices containing tunable dielectrics. The electrode technology is based upon a thick base metal layer to carry the high frequency high power signal, and a thin noble metal layer to provide the chemical compatibility and oxygen diffusion resistance needed during BST deposition. Tungsten is the ideal choice in this case due to its low thermal expansion coefficient, which allows thick layers to be prepared on a variety of substrates without delamination or hillock formation. IrO_x is the ideal noble metal layer given its ability to mitigate oxygen transport to the tungsten electrode core. BST thin films were successfully prepared on these electrode stacks, however, reduction of the oxygen flow rate during MOCVD depsotion was necessary. Electrical analysis suggests that this reduction in oxygen flow did not negatively impact the BST film quality. Tunabilities of 2:1, loss tangents of 0.007, and negligible dispersion between 100 Hz and 500 kHz were observed for the BST films. These numbers are consistent with many examples of BST thin films prepared on thin Pt surfaces thus represent a potential avenue for integrating thick metallization layers with tunable ferroelectric thin films. Finally, the ability to pattern and etch these hybrid electrodes using commonly available methods and chemicals at feature sizes consistent with RF and microwave devices was also shown. This suggests that this technology may be viable in a manufacturing environment.

Acknowledgments

The authors would like to acknowledge the support of NSF grant ECS-0113350, "Adaptive Integrated Radio Frequency Transceiver Front Ends for High Date Rate Wireless Communications", as well as the numerous discussions with Jayesh Nath of the North Carolina State University department of Electrical and Computer Engineering.

References

1. R.A. York, A.S. Nagra, P. Periaswamy, O. Auciello, and S.K. Streiffer, *J. Im, Int. Ferro*., **34**(1–4), 1617 (2001).
2. K. Bethe and F. Welz, *Mater. Res. Bull.*, **6**(4), 209 (1971).
3. D.C. Dube, J. Baborowski, P. Muralt, and N. Setter, *Appl. Phys. Lett.*, **74**(25), 3546 (1999).
4. H.N. Al-Shareef, K.D. Gifford, S.H. Rou, P.D. Hren, O. Auciello, and A.I. Kingon, *Integr. Ferroelectr.*, **3**(4), 321 (1993).
5. E.A. Brandes and G.B. Brook, in *Smithells Metals Reference Book*, 7th ed. (Butterworth and Heinemann, Oxford, England, 1992) Chap. 14.
6. T.B. Massalski, *Binary Alloy Phased Diagrams* (ASM International, U.S.A., 1996).
7. I. Barin and O. Knacke, *Thermochemical Properties of Inorganic Substances* (Springer-Verlag, Dusselforf, GDR, 1973).
8. S. Bilodeau et al., *Solid State Tech.*, **40**(7), 235 (1997).
9. C.B. Parker, J.-P. Maria, and A.I. Kingon, *Appl. Phys. Lett.*, **81**(2), 340 (2002).
10. G.T. Stauf, C. Ragaglia, J.F. Roeder, D. Vestyck, J.-P. Maria, T. Ayguavives, A. Kingon, A. Mortazawi, and A. Tombak, *Int. Ferro.*, **39**(1–4), 1271 (2001).